Control Algorithms of Propulsion Unit with Induction Motors for Electric Vehicle

Petr PALACKY, Pavel BRANDSTETTER, Petr CHLEBIS, Vaclav SLADECEK,
Petr SIMONIK, David SLIVKA
VSB - Technical University of Ostrava, 70833, Czech Republic
pavel.brandstetter@vsb.cz

***Abstract*—The article deals with the research of algorithms for controlling electronic differential and differential lock of an electrically driven vehicle. The simulation part addresses the development of algorithms suitable for the implementation into a real system of a road vehicle. The algorithms are then implemented into a vehicle, a propulsion unit of which is consists of two separate electric drives with induction motors fed by voltage inverters with own control units using advanced signal processors. Communication among control units is provided by means of SPI interface. A method of vector control is used for the control of induction motors. The developed algorithms are experimentally verified for correct function in a laboratory using a roll test stand and while driving an electrically driven vehicle on the road.**

***Index Terms*—electric drive, electric vehicle, induction motor, torque control, vector control.**

I. Introduction

Today, a mechanical differential can be virtually found in each type of a vehicle with combustion engine. The basic principle of mechanical differential is the distribution of torque supplied by a drive shaft to individual wheels so that the torque on all wheels is equal. However, for vehicles with the wheels driven by electric motors and not containing a mechanical differential, the development of algorithms for providing cooperation among electric motors by means of an electronic differential is required.

The functions of electronic differential (ED) are divided into basic and supplementary functions. The basic function is the distribution of the required torque to individual wheels. The supplementary functions include a differential lock, anti-slip function and anti-lock function during regenerative braking. In addition, a stabilization function of a vehicle may be added, which combines previous functions to ensure correct behavior of a vehicle under all conditions [1-8].

The subject of the research is a vehicle with an electrically driven front axle with the possibility for an independent torque/speed control of motors installed on the left and right wheel. The vehicle is equipped with two induction motors (IM) with integrated speed sensors and two voltage inverters with own control units. A battery provides the power. A vector control (VC) is used to give torque (or motor speed) control [9-16].

The communication among control units is an important part, because the development of electronic differential algorithm requires the exchange of immediate actual values of motor speed and torque. The SPI interface was selected as the main communication interface and the CAN busbar will be used to connect the drive unit of the vehicle to common communication busbar.

The article has been elaborated in the framework of the projects SP2014/119 and SP2014/203 which were supported by Student Grant Competition of VSB-Technical University of Ostrava, Czech Republic.

Digital Object Identifier 10.4316/AECE.2014.02012

II. List of the Used Symbols

$\boldsymbol{u}_S^S$	stator voltage space vector
$\boldsymbol{\psi}_R$	rotor flux vector
i_{Sx}, i_{Sy}	components of stator current space vector $\boldsymbol{i}_S^S$
i_m	magnetizing current
i_{Sxref}	reference value of the magnetizing component
i_{Syref}	reference value of the torque current component
ε	rotor angle
γ	angle of the vector rotation
$F_{IML,\,R}$	transfer function of left and right IM with VC
$F_{\omega L,\,R}$	transfer function of left and right speed controller
I_{LaRMS}	average RMS phase current of the left IM
I_{RaRMS}	average RMS phase current of the right IM
J_T	total moment of inertia
L_h	magnetizing inductance
$N_{WL,\,R}$	number of revolutions of the left and right wheel
$n_{WL,\,R}$	speed of the left and right wheel
n_L, n_R	speed of the left and right IM
o_T	tire circumference
$P_{L,\,R}$	power on the left and right wheel
R_Z	radius of the turn
$s_{L,\,R}$	length of travelled track - left and right wheel
s_V	length of travelled track - vehicle
$T_{L,\,R}$	torque of the left and right motor
T_{L_L}	load torque on the left wheel
T_{L_R}	load torque on the right wheel
$T_{ref\_L,\,R}$	required torque of the left and right motor
T_{ref_T}	total required torque
T_r	rotor time constant
T_S	torque on the drive shaft
T_T	total torque
t_V	time of cornering
$\omega_{L,\,R}$	angular speed of the left and right wheel
ω_m	real rotor angular speed
ω_{mref}	reference rotor angular speed

III. Function of the Mechanical Differential

The chapter deals with the introduction into the problem to be solved, with focus on a mechanical differential to serve later as a basis for the development of electronic differential algorithms in an electrically driven vehicle (EV).

Fixed coupling of the right and left wheel of the vehicle

ensures good control on straight sections of the road as well as in non-uniform adhesion conditions on individual wheels. The problem arises when the vehicle tracks through a corner, where a uniform shaft causes the wheels to slip, thus reducing the control of the vehicle. On the other hand, an independent movement of both wheels helps to better control the vehicle in corners; however, the problem arises when the wheels slip.

The basic principle of mechanical differential has changed very little since its invention in 1827. From mechanical point of view, it was endow with a number of other important functions, without which we could hardly imagine today's vehicles.

The mechanical differential enables to better control the vehicle in a corner, where the outer wheels travel a longer distance because they copy a greater radius than the inner wheels. If the wheels are on the same shaft, one or two wheels must slip, which, for example, leads to the reduced control of the vehicle. It is the difference in such revolutions of single-axle wheels that is handled by a differential gearing (differential). The differential is designed to automatically compensate for different revolutions of drive wheels when cornering and distribute the driving torque to both vehicle wheels at the same time [17-18].

From the point of view of the transmission of driving torques, there are the following versions of differential: without differential lock, with mechanical differential lock, differential with increased internal friction and limited slip differential.

The torque of drive shaft may be expressed by means of the torque of wheels as follows:

$$T_S = T_L + T_R \tag{1}$$

When cornering, the following equation must apply:

$$T_L = T_R = \frac{T_S}{2} \tag{2}$$

The outer wheel spins faster than the inner wheel, therefore $\omega_L \neq \omega_R$, and the power on the left and right side must be also different:

$$P_L = T_L \omega_L \,, P_R = T_R \omega_R \,, P_L \neq P_R \tag{3}$$

If we take into account the equation (2) in variable adhesion conditions on the left and right wheel (e.g. slippery or light surface), we can ascertain that in this case the equality of torque is inappropriate. The slipping wheel can have up to double revolutions than the differential cage and the differential should be put out of operation. This function is covered by a differential lock. For classical bevel-gear differential, the lock will couple in a defined way the differential cage and one bevel gear. The differential is put out of operation because the bevel pinions cannot also rotate. The self-locking types of differentials bring a disadvantage of the need for switching on and off the differential lock.

IV. Concept of Electric Vehicle

The basic concept of a vehicle with front wheel electrical drive is shown in Fig. 1. The front axle of a vehicle is driven by means of two self-contained drive units. Therefore, this is a vehicle with separate front axle wheel drive. All basic elements of electric drive units are situated in the front part of a vehicle, marked as left wheel drive unit (index L) and right wheel drive unit (index R). A battery (AB) is uniformly distributed along the entire vehicle. The meaning of used abbreviations is as follows: GB - gearbox with constant transmission, IM - induction motor, VI - voltage inverter and control unit, AB – battery.

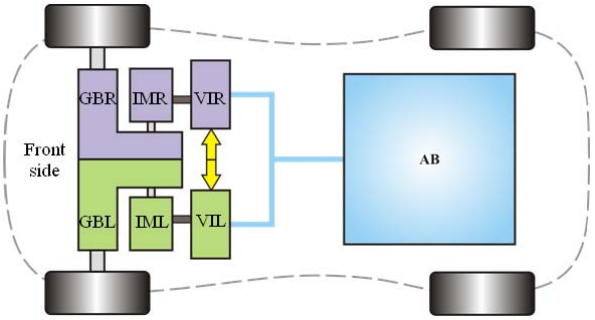

Figure 1. Basic concept of electric vehicle with front wheel drive

A gearbox is physically constructed as one piece, which contains two independent parts; the transmission ratio is constant and its value is $p = 6.01$.

A new concept of dual voltage inverter, consisting of two voltage inverters connected to one intermediate circuit and inserted in one chassis, is used in the vehicle.

V. Basic Analysis of the Real Electric Vehicle

For the basic analysis of the behaviour of a vehicle travelling in a corner, it is necessary to start from the concept of vehicle with the front axle being a drive axle with separate wheel drive. The point of intersection of the vehicle axis and the front axle axis marked as *A* (see Fig. 2) is selected as the reference point for simulations. When cornering, this point is distant from the centre of the turn *S* by radius R_Z. The distances of the right and left wheel from the centre of the turn are marked r_L and r_R.

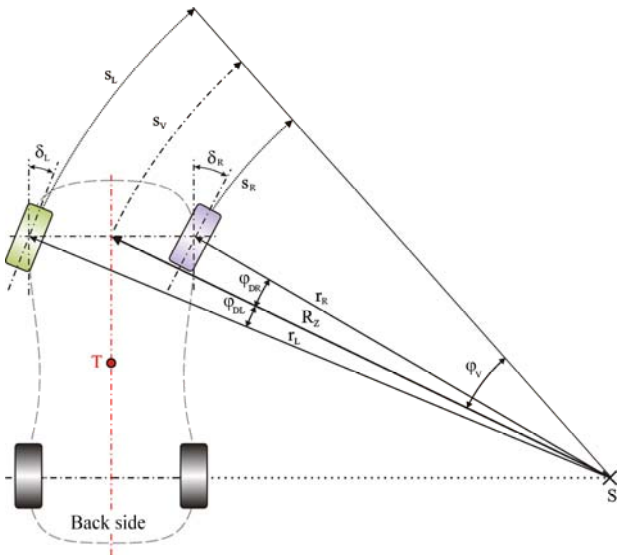

Figure 2. Kinematic model of the vehicle

When cornering, the vehicle travels a distance, which is calculated in relation to the track angle of the reference point φ_V. The track s_V is calculated as a circular sector with radius R_Z:

$$s_V = 2\pi R_Z \frac{\varphi_V}{360} \tag{4}$$

For individual wheels, the lengths of travelled tracks will be as follows:

$$s_L = 2\pi r_L \frac{\varphi_{DL}}{360}, s_R = 2\pi r_R \frac{\varphi_{DR}}{360} \quad (5)$$

If we use the standard size of a tire, e.g. 195/50 R15, we can calculate the number of revolutions of the individual wheels when cornering:

$$N_{WL} = \frac{s_L}{o_T}, N_{WR} = \frac{s_R}{o_T} \quad (6)$$

where o_T is the calculated tire circumference.

The speed of the individual wheels, if we know the time of cornering t_V, is calculated as follows:

$$n_{WL} = \frac{N_L}{60t_V}, n_{WR} = \frac{N_R}{60t_V} \quad (7)$$

The tracks or the revolutions of the left and right wheel in relation to the total track of the vehicle making a right-hand turn were calculated using the equations (4)-(7). The conditions of this situation were as follows: a) radius of the turn set to 3 metres, b) angle φ_V was set to 90°, c) size of tires 195/50 R15, d) distance of front axle wheel from vehicle axis was 0.86 m.

The graphical dependencies in Fig. 3 show that the tracks of the left and right wheel differ already in the half turn by 2.18 m. At the end of the turn, this difference is 2.93 m.

If we take into account the circumference of tire 1.81 m (for 195/50 R15), the difference in revolutions at the end of turn is 1.62 revolutions. This is a substantial difference, for the turn with radius 3 m, related to the total number of revolutions of wheels.

Fig. 4 shows the speeds of wheels depending on the speed of vehicle making a turn with radius 3 metre. With the speed of vehicle 10 kmh^{-1}, the difference in revolutions of the left and right wheel is 58.77 rpm. With increasing vehicle speed, with the same radius of the turn, the difference in revolutions of wheels increases linearly.

The behavior of vehicle without electronic differential with the control of *U*/*f* = const type was measured on the older type of vehicle. The two used induction motors were connected to the output of one voltage inverter, which means that the motors were fed by voltage with the same frequency.

The measurement was performed when making a right-hand turn with radius 3 m. One phase of each motor was measured. The *L* and *R* indices marking the left and right wheel are used in the characteristics.

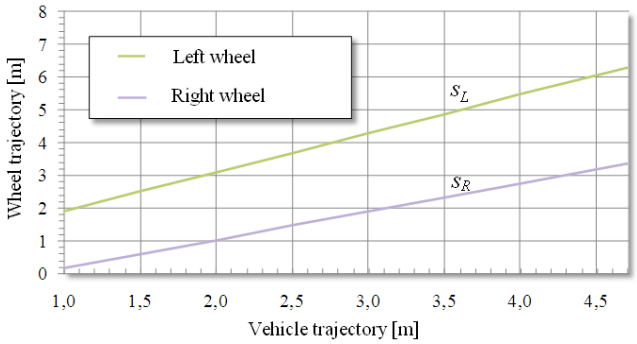

Figure 3. Dependencies of wheel trajectories on the vehicle trajectory, R_Z = 3 m

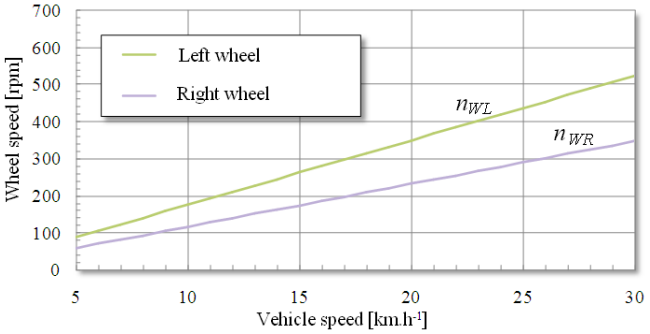

Figure 4. Dependencies of wheel speeds on the vehicle speed, R_Z = 3 m

As shown in Fig. 5, when driving a right-hand turn, there is a higher RMS value of current on the inner (i.e. right) wheel because this wheel must have higher slip.

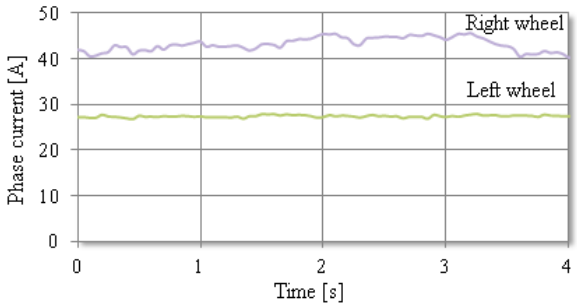

Figure 5. RMS values of the phase current, curve radius R_Z = 3 m (average RMS values of the current I_{RaRMS} =42.8 A, I_{LaRMS}=27.6 A)

This measurement shows the following:

a) The control of *U*/*f* = const type is not suitable for the use in an electrically driven vehicle, where the two motors are fed from one inverter, because with increasing slip the torque increases (in the stable part of torque characteristics), thus deteriorating the running properties.

b) Using a dual type of inverter with microcomputer control systems containing appropriate independent control of both motors will be a great benefit in terms of running properties and electricity consumption.

c) Using an electronic differential and other supplementary functions will be required.

VI. Electronic Differential

The basic function of electronic differential provides primary function, i.e. distribution of torque to the right and left wheel. When the vehicle is travelling in a straight section of the road, the same torques will be distributed to both wheels. The same will apply to cornering. The supplementary functions, which extend the basic function, are covered, for example, by a differential lock and electronic vehicle stabilization [19-22].

The electronic differential lock will be mainly used when driving in the field, on an icy road and other surfaces, where the non-uniform adhesion can cause the control of vehicle to reduce. It is required to start from the equality of speed or revolutions of individual wheels, which basically simulate coupled wheels of an axle.

The block diagram in Fig. 6 represents the control structure of electronic differential. The input value for the system is the total required torque, which can be compared to an accelerator pedal in a vehicle. The ED block divides

the total torque into the required torques of individual motors T_{ref_L}, T_{ref_R} according to the equation (2). By means of load torques T_{L_L}, T_{L_R} the load of individual motors is simulated when driving through a turn when the outer wheel is unloaded in the turn, while the inner wheel is loaded with the same amount of torque.

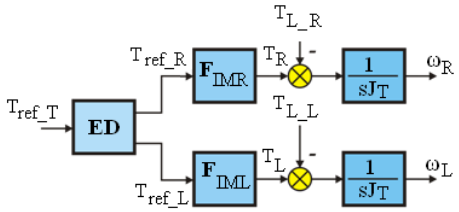

Figure 6. Block scheme of the electronic differential

During simulation, the same load torque was applied to both motors for the starting phase and the turn was simulated by changing this torque (see Fig. 7)

The basis of the ED lock model - Method 1 (see Fig. 8) involves motors with torque regulation and superior speed loop. The total required torque is again the input value for the system. This, together with actual torque of motors T_L, T_R, enters the block of total torque regulator CBM1, which is performed by I torque regulator, the output of which is the required revolutions of individual speed loops of motors.

In this model, a sudden change in the load torque is simulated, when the change in load torque on one wheel must initiate an opposite change on the other wheel, while the revolutions of both motors must not be changed in such situations.

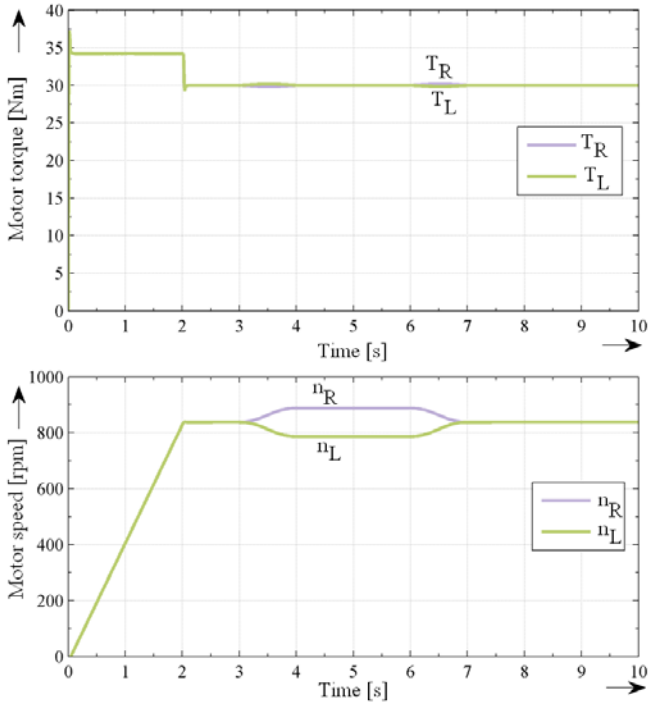

Figure 7. Simulation results of the ED on the vehicle driving through a turn

In the block CBM1, the torques T_L and T_R are subtracted from the required value of the total torque T_{ref_T}:

$$e_T = T_{ref\_T} - T_L - T_R \tag{8}$$

The regulation deviation e_T enters then the I-regulator with the limitation of maximum required speed.

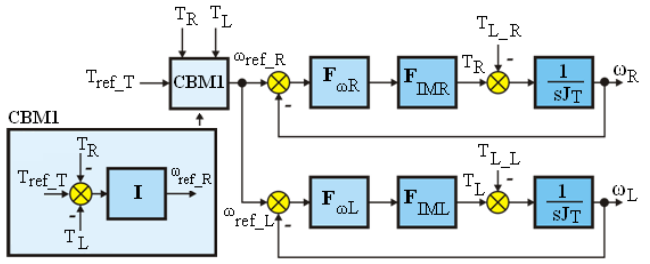

Figure 8. Block scheme of the electronic differential lock - Method 1

For the ED lock model - Method 2 (see Fig. 9), the first motor has only implemented the torque regulation and the other one contains additionally the superior speed loop.

The total required torque is again the input value for the system. This, together with actual torque of left motor T_L, enters the block of total torque regulator CBM2. The required torque of the right motor T_{ref_R} is the output of this block.

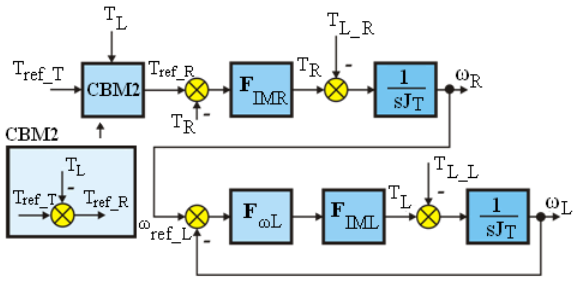

Figure 9. Block scheme of the electronic differential lock - Method 2

In the block CBM2, the torque T_L is subtracted from the required value of the total torque T_{ref_T}:

$$T_{ref\_R} = T_{ref\_T} - T_L \tag{9}$$

Fig. 10 and 11 show the behaviour of quantities of the two motors during step changes in load torques at the times t=4 s and t=7 s. The required value of the total torque T_{ref_T} is set to 35 Nm and at the time t=3 s reduced to 30 Nm.

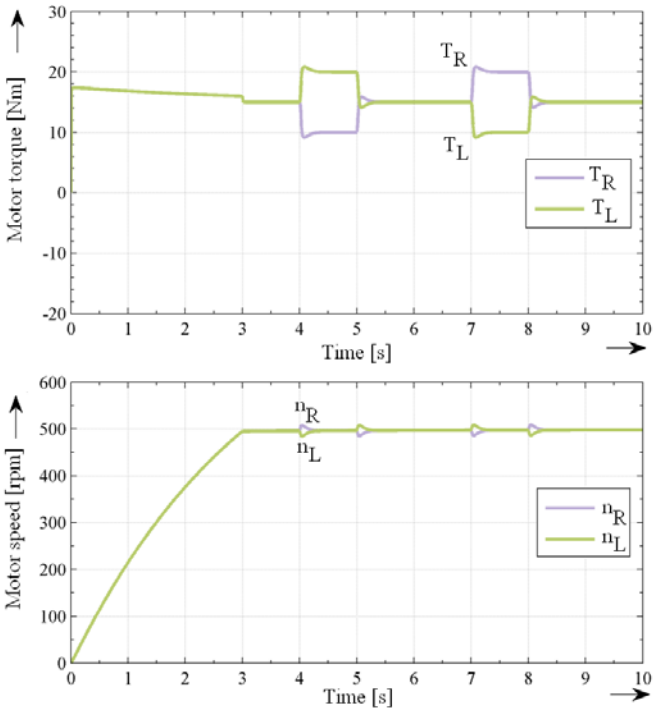

Figure 10. Simulation results the electronic differential lock at random disturbance, Method 1

As can be seen, the step change in load torques will give rise to transient phenomena in the characteristics of motor speed, the maximum difference in revolutions is 25 rpm (Method 1), or 16 rpm (Method 2) with the difference in load torques 10 Nm.

Simulation results of electric differential lock methods 1 and 2 confirmed theoretical assumptions. These methods will be further experimentally tested on real electrical vehicle which will use the propulsion unit with vector controlled induction motors.

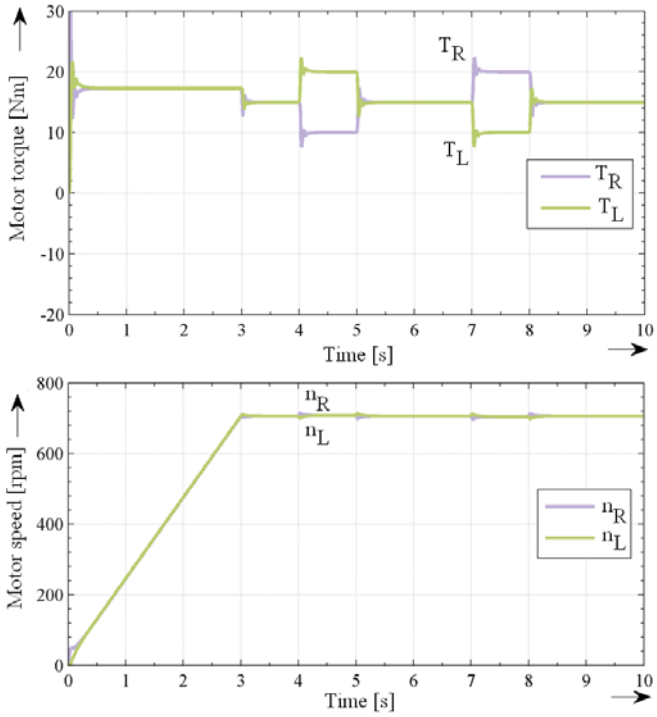

Figure 11. Simulation results the electronic differential lock at random disturbance, Method 2

VII. Control Structure of the Induction Motor Drive with Vector Control

The vector control of induction motor was selected for the reasons of the possibility to control both the torque and the revolutions. The advantage is the transition into a generator mode due to energy recovery back into the battery [16-16].

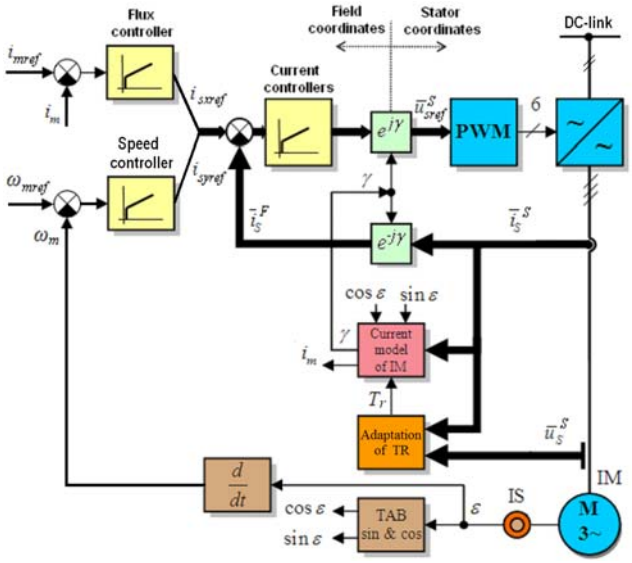

Figure 12. Control structure of the vector controlled induction motor

For variable speed electric drive with the induction motor, a cascade structure is often used because of its flexibility (see Fig. 12).

By using vector control, it is possible to control separately the flux producing component i_{Sx} and torque producing component i_{Sy} of the stator current vector $\boldsymbol{i}_S^S$ which is defined by stator phase currents. In reference to simple decoupling between individual magnetizing and torque current components i_{Sx}, i_{Sy}, it is useful to select a relative coordinate system [x, y], which rotates with angular speed ω_{im} and is oriented to the rotor flux vector $\boldsymbol{\psi}_R$. The rotor flux vector $\boldsymbol{\psi}_R$ is expressed by the magnetizing current i_m and the main induction of the induction motor L_h.

The cascade control structure consists of several control loops, whereas the current control loops for the magnetizing and torque current components i_{Sx}, i_{Sy} are subordinate and the flux and speed control loops are superior loops [23].

VIII. Realization of Propulsion Unit with Induction Motors

The basic concept of vehicle is described in Chapter IV. There are two mass-produced induction motors Siemens 1LA7 107-4AA with rated output 3 kW installed in a vehicle. The motors have jackets adapted to water cooling and the maximum output of 9 kW per motor is taken into account, i.e. triple overload. Induction motor parameters are listed in Tab. I.

TABLE I. PARAMETERS OF THE INDUCTION MACHINE

Parameter	Value
Rated power	3.0 kW
Rated speed	1420 rpm
Rated voltage	230 V/400 V
Rated current	6.4 A
Rated torque	20.2 Nm
Number of pole-pairs	2
Moment of inertia	0.0058 kgm^2

The induction motors are powered by a dual voltage inverter made at the Department of Electronics. Switching elements are IGBTs SK200GD066T; U_{CE}=600V; I_C=200A; and drivers are Skyper 32.

The battery consists of LiFePO4 accumulators with voltage 3.2 V and nominal capacity 40 Ah. The total battery voltage is 320 V.

In the control systems, a Freescale DSP 56F8037 digital signal processor is used. The intercommunication of drive units of the left and right wheel is required for the implementation of ED. This function will be covered by an electronic differential control unit (EDCU), which receives the actual values of torque and speed of motors from their control systems CSL, CSR and according to algorithms, the unit sends back the new required values of quantities.

The EDCU can be a self-contained control unit or it can be implemented as an algorithm included in the code within one of the control systems CSL, CSR. The concept of the second type is used for the implementation, when one control system is the master system and the other is the slave system.

A control unit for supplementary functions of vehicle stabilization can be added to ED, which uses the signals of other sensors (steering wheel turn sensor, longitudinal and

side acceleration sensor) to correct the ED function. The communication interface is used for the connection to an on-board unit of the vehicle [24].

IX. Experimental Results

Once the control algorithms of the induction motor vector control and the communication via the SPI interface have been verified, the functions of ED and ED lock were verified according to the indicated methods 1 and 2. The measurement was first performed on a roll brake test stand (see Fig. 13) in several modes and then on the road in different situations: straight start, left-hand turn, right-hand turn, reversing, straight start with regenerative braking. The measuring card NI DAQCARD-6024E in connection with a laptop was used for the recording of quantities. The results were then plotted in graphs [24].

Figure 13. ED testing on the roll brake test stand

The maximum total required torque was set to T_{ref_T} = 120 Nm. The voltage inverters were supplied by a vehicle battery with nominal voltage 320 V.

Fig. 14 shows the start of vehicle with the ED by means of the vector control, where the maximum total required torque was set to T_{ref_T} = 120 Nm and the rate of rise was limited using a ramp. The vehicle starts at the time t = 2 s and the speed of both motors increases. The accelerator pedal is applied at the time t = 8.8 s and the speed starts decreasing, the mechanical brakes are applied. Furthermore, the algorithm is switched over at the time t = 14 s followed by vehicle reversing.

Fig. 15 shows the situation when the vehicle starts on the straight section of the road and then makes a right-hand turn. The characteristics of motor speed show that the speed of the right motor driving the inner wheel starts reducing when making a turn, while the speed of the left motor driving the outer wheel starts increasing.

The electronic differential running on the vector control implemented according to the equation (2) functions smoothly in all tested situations. The vector control algorithm is at the same time applicable to the regenerative braking of induction motors and allows also motor de-excitation.

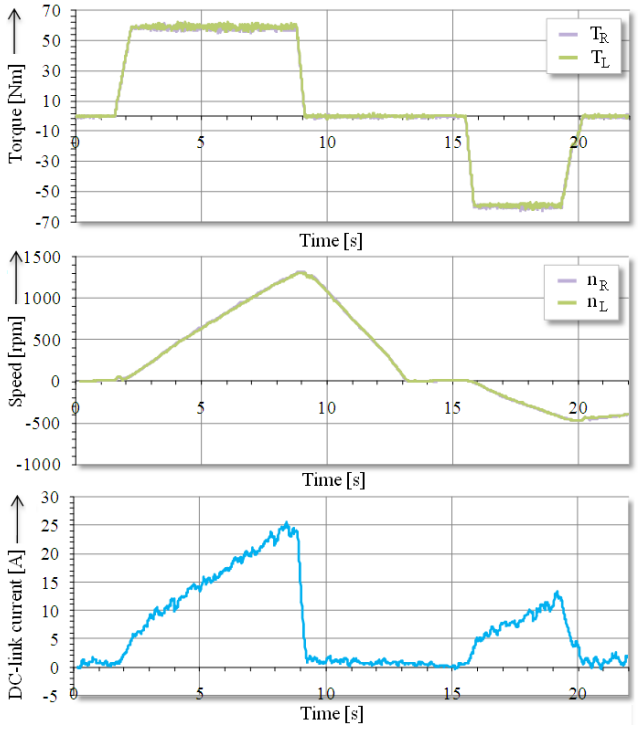

Figure 14. Operation of the ED - start and reversing EV

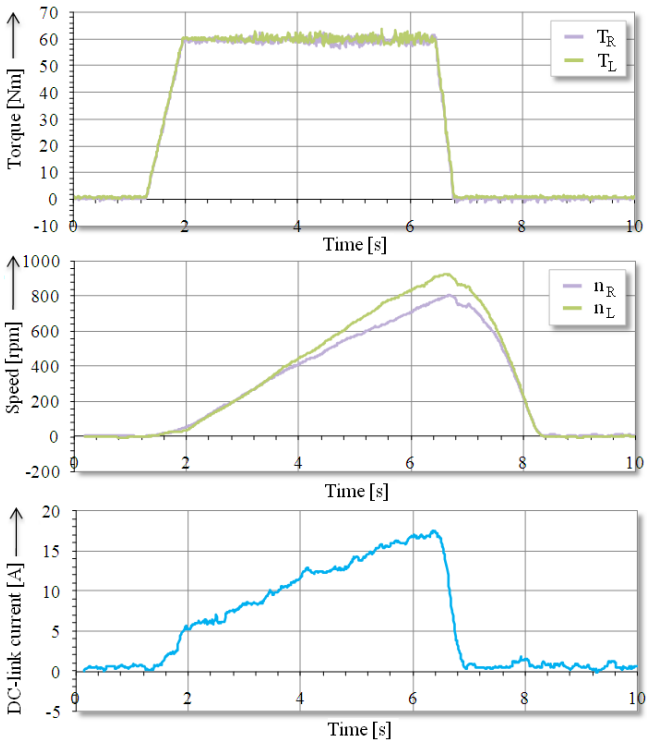

Figure 15. Operation of the ED - start and right-hand turn

The methods of electronic differential locking were implemented into the vector control algorithm and first verified by placing the right wheel of vehicle on a roll dynamometer and supporting the other one to rotate freely. Several situations were verified to draw the behavior of individual methods.

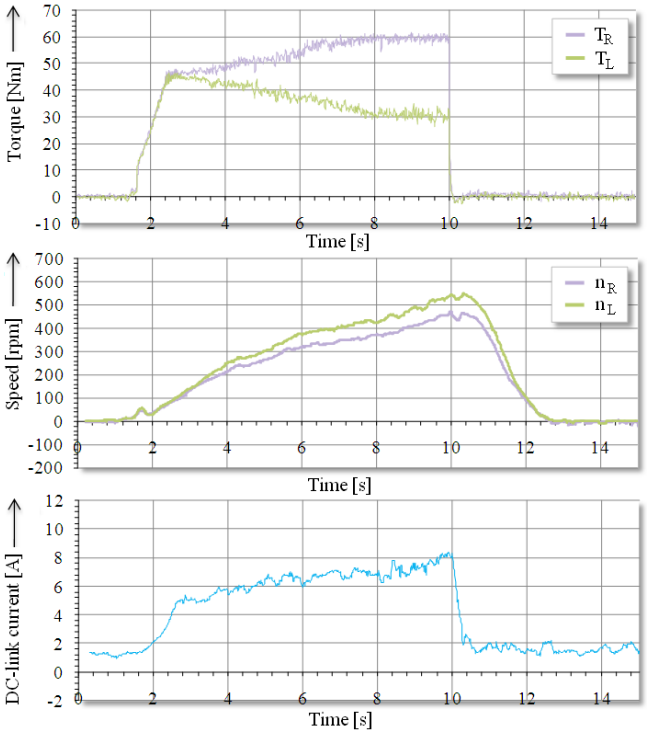

Figure 16. Operation of the ED lock - start and right-hand turn, Method 1

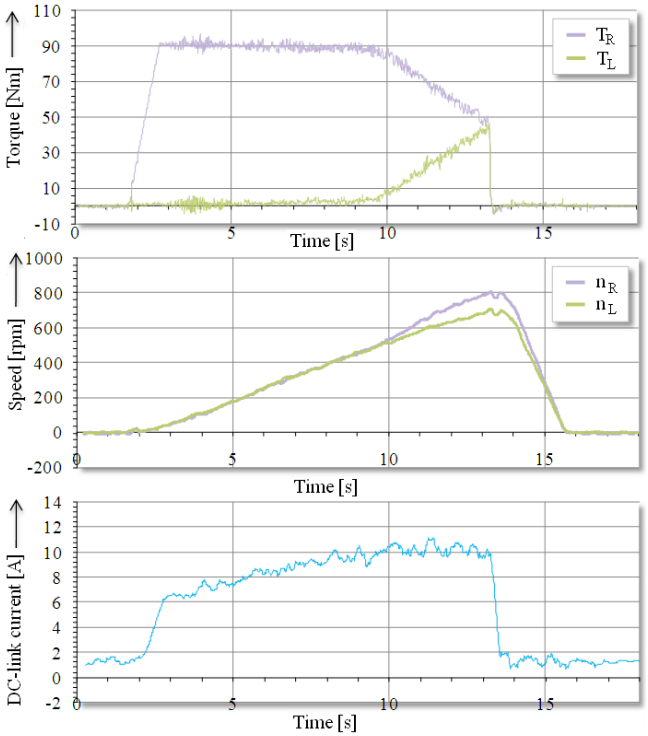

Figure 17. Operation of the ED lock - start and left-hand turn, Method 2

In addition, the two methods of ED locking were tested on the road. The verification of the methods of ED locking on the road confirmed the conclusions drawn from the measurement on a roll dynamometer. The maximum total required torque was set to T_{ref_T} = 90 Nm. The voltage inverters were supplied by a vehicle battery with nominal voltage 320 V.

When making a right-hand turn, the ED lock functions according to the Method 1 by applying lower torque to the motor of the outer wheel (index L) than to the motor of the inner wheel (see Fig. 16).

When making a left-hand turn at the time t = 9.5 s, the ED lock distributes, according to the Method 2, the torques, when decreasing the torque applied to the motor of the outer wheel (index R), thus increasing the torque of the motor of the inner wheel (index L). This distribution of torques is based on the equation (9) (see Fig. 17).

For the Method 1, the torqueses are uniformly distributed in normal situation to both motors of wheels, contrary to the Method 2, when the total required torque is transmitted only to the motor of one wheel. For the Method 1, a speed overshoot occurs on freely rotating wheel. However, as ascertained from the behavior of both methods on the road, the two methods are usable as electronic differential lock in an electrically driven vehicle [24].

X. Conclusion

The article deals with the implementation of the electronic differential function in a vehicle with an independent front axle wheel drive, covered by an electric drive. The basic analysis of the function of mechanical differential was performed, which was used as a basis for the development of simulation models of the electronic differential and selected supplementary functions. These models were subsequently implemented into the drive control algorithm of a real vehicle. The suggested control algorithms were verified in real conditions.

The measurement on the older type of a vehicle equipped with one voltage inverter, which supplies both induction motors of the front axle with the control ensuring constant magnetic flux of the machine (U/f = const) ascertained that this method is not suitable in terms of vehicle control and electricity consumption. A new concept of a double voltage inverter with control units allowing an independent control of speed/torque of both motors was used, which is clearly beneficial to the improvement of dynamic behavior and consumption of this vehicle.

For the control of induction motors, the method of vector control was selected, which allows the transition into a generator mode of the machine, taking into account the subsequent energy recovery back to the battery. The control methods were implemented into the control system with DSP Freescale 56F8037.

Furthermore, one of the supplementary functions, specifically the differential lock, was implemented. Two methods implementing this function were developed and experimentally verified. The conclusions may be drawn from the behavior of a vehicle on the road that both methods are usable as the ED locks in an electrically driven vehicle.

For the function of regenerative braking, the identification of the moment when this function should be activated and deactivated is important. The use of the function of regenerative braking would appear to be more appropriate in the city traffic, because the frequent and intensive application of mechanical brakes would be avoided. This would lead to the lower wear of the vehicle brake system. The consumption of energy is on the other hand. When activating the function of electric brake, the regenerative braking occurs first, followed by back-current braking, which consumes the power supplied by the battery.

The unquestionable advantage of an electrically driven vehicle is the dynamic aspect of the entire system, where the

moment of inertia is lower than the moment of inertia of a classical combustion engine vehicle, because for electric motor, the required changes in the moment become evident with the minimum delay.

REFERENCES

[1] B. K. Bose, "Global Energy Scenario and Impact of Power Electronics in 21st Century," IEEE Transactions on Industrial Electronics, vol. 60, no. 7, pp.2638-2651, 2013.

[2] L. G. Lu, XB. Han, JQ. Li, JF. Hua, MG. Ouyang, "A Review on the Key Issues for Lithium-Ion Battery Management in Electric Vehicles," Journal of Power Sources, vol. 226, pp. 272-288, 2013.

[3] Y. Liu, J. Zhao, R. Wang, CG. Huang, "Performance Improvement of Induction Motor Current Controllers in Field-Weakening Region for Electric Vehicles," IEEE Transactions on Power Electronics, vol. 28, no. 5, pp. 2468-2482, 2013.

[4] S. Haghbin, K. Khan, S. Zhao, M. Alakula, S. Lundmark, O. Carlson, "An Integrated 20-kW Motor Drive and Isolated Battery Charger for Plug-In Vehicles," IEEE Transactions on Power Electronics, vol. 28, no. 8, pp. 4013-4029, 2013.

[5] D. Hamza, M. Pahlevaninezhad, P. K. Jain, "Implementation of a Novel Digital Active EMI Technique in a DSP-Based DC-DC Digital Controller Used in Electric Vehicle (EV)," IEEE Transactions on Power Electronics, vol. 28, no. 7, pp. 3126-3137, 2013.

[6] P. Fedor, D. Perdukova, "Energy Optimization of a Dynamic System Controller," in Proc. International Joint Conference CISIS'12-ICEUTE'12-SOCO'12 Special Sessions, Book Series: Advances in Intelligent Systems and Computing, vol. 189, pp. 361-369, 2013.

[7] K. Hartani, Y. Miloud, A. Miloudi, "Improved Direct Torque Control of Permanent Magnet Synchronous Electrical Vehicle Motor with Proportional-Integral Resistance Estimator," Journal of Electrical Engineering & Technology, vol. 5, no. 3, pp. 451-461, 2010.

[8] A. Nasri, A. Hazzab, I. K. Bousserhane, S. Hadjeri, P. Sicard, "Fuzzy Logic Speed Control Stability Improvement of Lightweight Electric Vehicle Drive," Journal of Electrical Engineering & Technology, vol. 5, no. 1, pp. 129-139, 2010.

[9] P. Matic, S. N. Vukosavic, "Speed Regulated Continuous DTC Induction Motor Drive in Field Weakening," Advances in Electrical and Computer Engineering, vol. 11, issue 1, pp. 97-102, 2011. [Online]. Available: http:// dx.doi.org/10.4316/AECE.2011.01016

[10] J. Vittek, V. Vavrus, P. Bris, L. Gorel, "Forced Dynamics Control of the Elastic Joint Drive with Single Rotor Position Sensor," Automatika, vol. 54, issue 3, pp. 337-347, 2013.

[11] D. M. Stojic, "An Algorithm for Induction Motor Stator Flux Estimation," Advances in Electrical and Computer Engineering, vol. 12, issue 3, pp. 47-52, 2012. [Online]. Available: http:// dx.doi.org/10.4316/AECE.2012.03007

[12] D. Milicevic, V. Katic, Z. Corba, M. Greconici, "New Space Vector Selection Scheme for VSI Supplied Dual Three-Phase Induction Machine," Advances in Electrical and Computer Engineering, vol.13, issue 1, pp. 59-64, 2013. [Online]. Available: http:// dx.doi.org/10.4316/AECE.2013.01010

[13] P. Zaskalicky, B. Dobrucky, "Complex Fourier Series Mathematical Model of a Three-Phase Inverter with Improved PWM Output Voltage Control," Elektronika Ir Elektrotechnika, issue 7, pp. 65-68, 2012.

[14] P. Spanik, M. Frivaldsky, P. Drgona, J. Kandrac, "Efficiency Increase of Switched Mode Power Supply through Optimization of Transistor´s Commutation Mode", Elektronika Ir Elektrotechnika, issue 9, pp. 49-52, 2010.

[15] J. Gacho, M. Zalman, "IM Based Speed Servodrive with Luenberger Observer," Journal of Electrical Engineering - Elektrotechnicky Casopis, vol. 61, issue 3, pp. 149-156, 2010.

[16] V. Smidl, Z.Peroutka, "Advantages of Square-Root Extended Kalman Filter for Sensorless Control of AC Drives," IEEE Transactions on Industrial Electronics, vol. 59, issue 11, pp. 4189-4196, 2012.

[17] R. Rajamani, Vehicle Dynamics and Control. London: Springer Verlag, 492 p., 2012.

[18] K. Kiencke, L. Nielsen, Automotive Control Systems. Berlin: Springer-Verlag, 2nd ed., 512 p., 2005.

[19] FK. Wu, T.J. Yeh, CF. Huang, "Motor control and torque coordination of an electric vehicle actuated by two in-wheel motors," Mechatronics, vol. 23, no. 1, pp. 46-60, 2013.

[20] N. Bouchetata, M. Bourahla, L. Ghaouti, "Behavior Modeling and Simulation of Double Wheeled Electric Vehicle Drive," Przeglad Elektrotechniczny, vol. 88, no. 10A, pp. 218-223, 2012.

[21] S. You, H. Lee, D. Lee, H. Mok, Y. Lee, S. Han, "Speed Ratio Control for Electronic Differentials," Electronics Letters, vol. 47, no. 16, pp. 933-934, 2011.

[22] Y. Zhou, SJ. Li, XQ. Zhou, ZD. Fang, "The Control Strategy of Electronic Differential for EV with Four In-wheel Motors," in Proc. 2010 Chinese Control and Decision Conference, vols. 1-5, pp. 4190-4195, 2010.

[23] P. Brandstetter, A.C. Controlled Drives - Modern Control Methods. Monograph, VSB-Technical University of Ostrava, 1999.

[24] D. Slivka, "Control Methods of an Induction Motor in Vehicle Drive Unit," PhD Thesis, Dept. of Electronics, VSB-Technical University of Ostrava, Czech Republic, 2012.